Commentary

Why are so many adhesive pads hairy?

Walter Federle

Department of Zoology, University of Cambridge, Downing Street, Cambridge CB2 3EJ, UK

e-mail: wf222@cam.ac.uk

Summary

Many arthropods and vertebrates possess tarsal adhesive pads densely covered with setae. The striking morphological convergence of 'hairy' pads in lizards, spiders and several insect orders demonstrates the advantage of this design for substrate adhesion. Early functional explanations of hairy adhesive organs focused on the performance on rough substrates, where flexible setae can make more intimate contact. Recent theoretical and experimental work shows that the hairy design can also help to achieve self-cleaning properties, controllable detachment and increased adhesion. Several arguments have been proposed to explain why adhesive forces are maximised. First, the 'Force scaling' hypothesis states that when adhesive forces scale linearly with the dimensions of the contact, adhesion is increased by dividing the contact zone into many microscopic subunits. Second, the 'Fracture mechanics' argument implies that adhesion is maximised when the size of adhesive contacts is smaller than the critical crack length. Third, the 'Work of adhesion' model suggests that adhesion increases due to the bending and stretching of setae and associated energy losses during detachment.

Several morphological traits of hairy adhesive pads can be explained by the need to maximise the work of adhesion, while avoiding the sticking of setae to each other (self-matting). Firstly, if setae are oblique and convex toward the foot tip as typical of most hairy pads, arrays should achieve greater adhesion. Secondly, a branched seta morphology not only confers the advantage that setae can adapt to roughness at different length scales but also prevents self-matting and increases the work of adhesion.

It is predicted from the 'Work of adhesion' model that adhesion of pads with unbranched setae cannot be increased by subdividing the contact zone into ever finer subcontacts, because this would increasingly cause self-matting. However, contact splitting can increase adhesion if setae are branched. The greater density of setae in large animals has been interpreted by 'Force scaling'. However, the existing data can be explained by the effect of seta branching and by a fundamental difference between 'wet' and 'dry' adhesive systems. As insects employ adhesive fluids, they can cope with small-scale surface roughness even with relatively blunt seta tips, whereas the dry systems of lizards and spiders require extremely fine endings.

Key words: adhesive setae, biomechanics, animal adhesion, fibrillar adhesion, contact mechanics, branching.

Introduction

"*The foot of a fly is a most admirable and curious contrivance, for by this the flies are enabled to walk against the sides of glass, perpendicularly upwards, and to contain themselves in that posture long as they please; nay, to walk and suspend themselves against the undersurface of many bodies, as the ceiling of a room, or the like...*" Hooke, R. (1665).

Many animals that live on trees or regularly visit plants have evolved adhesive organs on their feet. Despite the wide diversity of animals using adhesion and the variety of structures employed, tarsal adhesive organs come in only two basic designs: (1) pads with a relatively smooth surface profile and (2) pads densely covered with specialised, μm- or nm-sized setae. 'Hairy' adhesive organs have evolved independently at least three times in lizards (Irschick et al., 1996; Williams and Peterson, 1982), at least three times in insects (Beutel and Gorb, 2001), and occur in three phylogenetically distant groups of spiders (Coddington and Levi, 1991; Rovner, 1978). This suggests that hairy pads represent an optimised design for surface attachment. What is the advantage of this convergently developed morphology?

No later than in the 17th century, the pioneers of light microscopy were intrigued by the highly regular structures of fly feet and speculated about their function (Hooke, 1665; Power, 1664). Adhesive hairs were thought to work by interlocking with microscopic protrusions of the substrate.

However, later observations aided by scanning electron microscopy showed that hairy pads perform well on perfectly smooth substrates, where setae cannot interlock. Clearly, the contact area of a hairy pad on a smooth substrate is smaller than that of an equal-sized smooth adhesive pad (as found in many insect orders and treefrogs). Assuming that adhesive forces are proportional to contact area (e.g. Stork, 1980a; Walker et al., 1985), the hairy pad morphology should reduce rather than enhance adhesion, an apparent contradiction that had not been addressed until recently.

Advantages of hairy pad design

Several recent studies, both experimental and theoretical, demonstrate that a 'hairy' pad design can convey a number of advantages.

(1) Rough surface compatibility

Adhesion between rough solids is in most cases strongly reduced due to the loss of effective contact area (Fuller and Tabor, 1975). This loss can be compensated if at least one of the adherends is very soft (Briggs and Briscoe, 1977). Hairy adhesive pads easily adapt to the topography of rough substrates and achieve intimate contact. Smooth pads are also able to replicate the surface profile (Gorb et al., 2000) but only at the cost of using very soft materials, which are typically more susceptible to creep, degradation (wear) and contamination. Due to the bending and stretching of setae and the flexibility of very thin seta end plates, arrays of adhesive setae behave like very soft solids (i.e. they achieve a low effective elastic modulus) even though they are made of relatively hard materials (see Appendix) (Glassmaker et al., 2004; Persson, 2003). Very fine setae not only result in a low effective elastic modulus but also have the advantage that their μm- or nm-sized tips can make contact with small-scale surface roughness. Intimate surface contact not only increases adhesion but also frictional forces, which are essential for climbing animals.

(2) Self-cleaning capacity

All animals employing sticky adhesive pads on their feet must have ways to keep them clean. A hairy pad morphology may be less susceptible to contamination and can even have self-cleaning properties (Hansen and Autumn, 2005). In fact, geckos are capable of keeping their toe pads sticky without any active grooming. This effect has been explained by the greater adhesion of dirt particles to the substrate than to the very fine tips of gecko spatulae (Hansen and Autumn, 2005). Thus, dirt particles are removed from the setae with every single step. Self-cleaning is facilitated for setae of relatively hard, non-tacky materials with a low surface energy (Hansen and Autumn, 2005). Even though many insects spend much of their life time grooming themselves (Dawkins and Dawkins, 1976; Farish, 1972; Lefebvre, 1981), self-cleaning may also be an important component of recycling adhesive capability.

(3) Effortless and controllable detachment

Gecko setae were observed to generate large detachment forces only when they had been slightly pulled in the proximal direction with a small preload (Autumn et al., 2000). Setae adhered well when their angle with the substrate was smaller than a critical value of ca. 30°, but detached at larger angles. This behaviour is related to the asymmetrical structure of the seta tip and has been confirmed by a finite element model (Gao et al., 2005). The angle- and direction-dependent adhesion of setae is very important because it helps animals to switch easily between attachment and detachment by performing gross leg movements toward the body or away from it (see below, Fig. 2). As a consequence, vertically climbing geckos do not generate any appreciable normal forces associated with attachment or detachment (Autumn and Peattie, 2002).

(4) Maximised adhesion

Despite the smaller contact area, a hairy pad morphology may in fact maximise adhesion, even on a smooth substrate. This effect has been confirmed experimentally (Hui et al., 2004; Peressadko and Gorb, 2004) and will be discussed in the following sections.

Rough surface compatibility, self-cleaning, controllable detachment and maximised adhesion are essential for the biological function of adhesive pads. Achieving similar properties would be highly desirable for man-made technical adhesives. Technical adhesives are usually not or only slowly detachable, not controllable and susceptible to contamination (de Crevoisier et al., 1999; Khongtong and Ferguson, 2002). Consequently, the biomimetic fabrication of fibrillar adhesives has excited much interest over the last years (Autumn et al., 2002; Geim et al., 2003; Hui et al., 2004; Northen and Turner, 2005; Sitti and Fearing, 2003; Yurdumakan et al., 2005). A wide range of applications is conceivable for these novel fibrillar adhesives, including micro- and nanomanipulation in production processes, microelectronics, biomedicine and robotics (Paine, 2000).

Morphology and design constraints for hairy adhesive pads

Adhesive hairs in insects, spiders and lizards are strikingly similar in morphology (Stork, 1983b). Setae represent hypertrophied structures of the outer epidermis in lizards (Ruibal and Ernst, 1965). Arthropods possess hollow setae with sockets (in spiders, beetles and earwigs) or without sockets (in flies). All setae are elongate structures with high aspect ratios ranging from 10 to 80 (Gorb, 2001; Haas and Gorb, 2004; Williams and Peterson, 1982). Adhesive setae from all taxonomic groups regularly bear special terminal elements, which are very thin and range in contact area from ca. 0.04 to 50 μm^2 (Arzt et al., 2003; Persson and Gorb, 2003; Stork, 1980b). These terminal elements can have very different shapes (often on the same tarsus) ranging from longitudinal, undifferentiated hair tips to broadened triangular and circular end-plates, often with a concave surface and a bulged rim

(Haas and Gorb, 2004; Langer et al., 2004). In hairy pads of insects, adhesion is mediated by a liquid secretion, which is released from gland pores at the base of the setae [e.g. in beetles (Betz, 2003)] or, in some cases, from an opening under the end-plate at the tip of the hollow adhesive hair (Gorb, 1998). No fluid secretion appears to be present in spiders and lizards.

Both in lizards and insects, the complexity of setae was found to be greater toward the distal side of the tarsus (Niederegger et al., 2002; Stork, 1983b). Setae of most insects and of anoline and scincid lizards (Williams and Peterson, 1982) are unbranched and only bear a single terminal element. By contrast, some beetles as well as spiders and geckonid lizards possess branched setae. The branched morphology can originate from the differentiation of cuticle (in spiders) or from the aggregation of many fibers to larger functional units, as in geckos (Stork, 1983b).

Seta density and self-matting

In the course of evolution, several functional constraints may have shaped the morphology of hairy adhesive pads. Apart from the requirements of flexibility and adhesive strength, the setae have to be designed in a way that they avoid fracturing and sticking to each other (Spolenak et al., 2005). The latter constraint is particularly important, because it imposes a limit to setal density and seta miniaturisation (Stork, 1983a). Setae stuck together at their tips are frequently observed in dried specimens of hairy adhesive pads, suggesting that many adhesive pads are designed close to the limit of 'self-matting' [also termed 'lateral collapse' (Glassmaker et al., 2004) and 'condensation' (Persson, 2003)]. Conditions for the self-matting of setae have been derived from bending beam models by several authors (Glassmaker et al., 2004; Persson, 2003; Sitti and Fearing, 2003; Spolenak et al., 2005). The model by Sitti and Fearing assumes the seta tips stick to each other with the same force F_0 with which they adhere to the surface (Sitti and Fearing, 2003). If d is the minimum possible distance between two setae, where self-matting does not yet occur, the maximum setal density N_A (i.e. the number of setae per unit pad area) is given by:

$$N_A \cong \frac{1}{d^2} \leqslant \frac{9\pi^2 r^8 E^2}{64 F_0^2 l^6} , \qquad (1)$$

where E is the elastic modulus, r and l the radius and length of the seta, respectively. If setae are unbranched, N_A can only be increased by reducing the length of the setae and/or by using a harder seta material (Eqn 14). This in turn will make hairy pads less compliant and will reduce the array's work of adhesion.

Several aspects in the morphology of adhesive setae may be explained by the requirement to reduce self-matting, which is obviously detrimental to adhesive function. Seta tips appear to be designed in a way that adhesion is maximised on one side of the tip (i.e. on the side that acts as adhesive contact area) whereas it is minimised on the lateral and dorsal faces so as to avoid the sticking of setae to each other. Between-seta adhesion may also be reduced due to the cylindrical shape of the seta stalks (Glassmaker et al., 2004), or due to small nodules, protusions and corrugations on the dorsal surface of setal tips in various insects (Fig. 2A) (Haas and Gorb, 2004; Stork, 1983b). These factors reduce the contact area between neighbouring setae. Moreover, I propose that perhaps the most effective way to prevent self-matting is the branched seta morphology found in spiders (Foelix, 1982) and geckos (Ruibal and Ernst, 1965) and some beetles (Stork, 1980b), because individual spatulae (i.e. the terminal branches) are effectively shorter and attractive forces between neighboring setae will be reduced due to the small number of contacting spatulae (see Appendix).

Angle and curvature of setae

An important factor that distinguishes animal adhesive setae from the first generation of microfabricated biomimetic fibrillar adhesives (Geim et al., 2003; Hui et al., 2004; Peressadko and Gorb, 2004) is the fact that they are not perpendicular and usually possess some degree of curvature. Setae are almost always slightly oblique, with the seta tips oriented in the distal leg direction. This has the effect that a pull of the leg toward the body (which occurs when the animal is walking upside down) will not compress and buckle the setae but set them under tension. The skewness of the setae strongly increases their flexibility in the perpendicular direction and therefore the ability of the setal array to conform to rough substrates (Eqn 8) (Glassmaker et al., 2004). A seta angle smaller than 90° will also result in a considerable increase of the seta's detachment energy and the work of adhesion of the setal array (see Appendix).

Since sloped setae come closer to each other than perpendicular ones, they may need to be spaced further apart in order to avoid self-matting. Seta spacing in hairy pads of some insects indeed shows the predicted direction-dependence. In *Coccinella septempunctata*, setae stand closer within horizontal rows but further apart in the direction perpendicular to it (Fig. 1A). Similar patterns appear to be present in flies [see figures in Niederegger et al. (Niederegger et al., 2002)]. The lateral deflection of setae (i.e. perpendicular to the plane of the slope) is often limited by the construction of the socket and by a flattened cross section of the seta, which is thinner along the proximal-distal axis of the tarsus (e.g. Eisner and Aneshansley, 2000; Haas and Gorb, 2004). As a consequence of the wider spacing of setae in the direction of the slope, it can be predicted that the work of adhesion is maximal for an intermediate seta angle of ca. 35° (Fig. 1B, derivation see Appendix). This angle is smaller than naturally occuring fiber angles (Gao et al., 2005; Haas and Gorb, 2004). Overly flat adhesive setae may have the disadvantage that they can no longer make contact to steeper parts of a rough surface topography. Fig. 1B shows that even slightly sloped setae (as found in most systems) lead to significantly greater adhesion.

Increased displacement and work of adhesion may be achieved not only by making the fibers oblique but also by
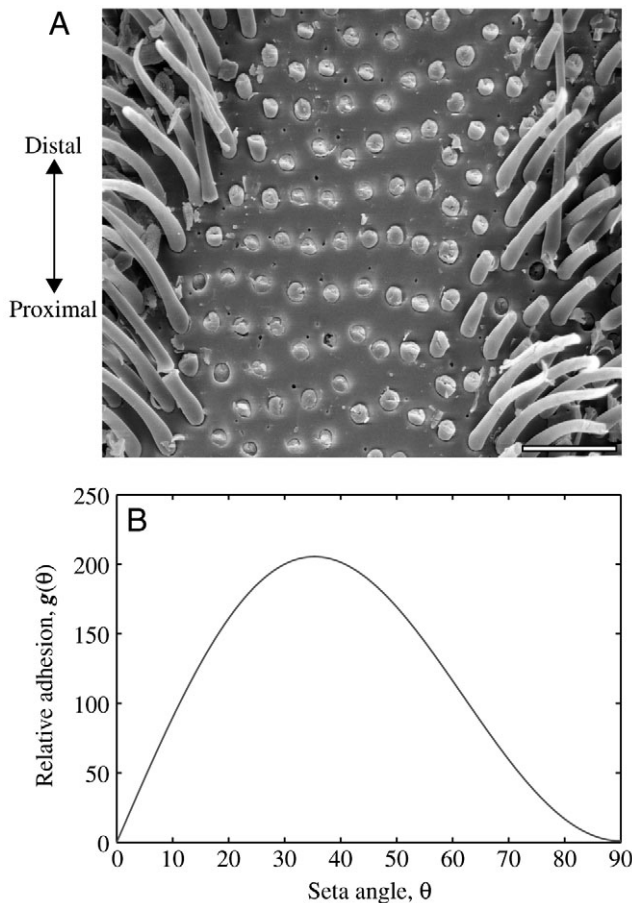
Fig. 1. (A) Ventral view of first tarsal segment of the ladybird *Coccinella septempunctata* (setae scratched away in the center to show the underlying cuticle. Note that setae stand in rows; the distance in the proximal-distal direction is greater than perpendicular to it. Scale bar, 20 μm. (B) Relationship between pad adhesion (work of adhesion of a setal array) and seta angle, as predicted from the Work of adhesion model and the assumption that sloped setae must be spaced further apart in the direction of the slope to avoid self-matting [function $g(\theta)$ of Eqn 10 (see Appendix), plotted here for a seta aspect ratio ($l/2r$) of 10].

giving them some degree of curvature (Persson, 2003). When setae are curved in the proximal-distal direction, there are two possible orientations, with the seta stalks being convex toward either the distal or the proximal side (Fig. 2). Available side-views of setae in various animal groups bearing adhesive setae show that setae are typically convex toward the distal side [Dermaptera (Haas and Gorb, 2004), Coleoptera (Fig. 2A); (Eisner and Aneshansley, 2000), Strepsiptera (Pohl and Beutel, 2004) and geckos (Gao et al., 2005)]. Two functional reasons are proposed for this particular curvature orientation. First, and most importantly, this design gives rise to the controllability of attachment and detachment. Seta tips in the 'default' (non-contact) position are often not parallel to the substrate, and sometimes even perpendicular, with the ventral contact zones facing toward the body [e.g. see seta figures published elsewhere (Eisner and Aneshansley, 2000; Gao et al., 2005;

Haas and Gorb, 2004)]. Setae can only adhere significantly when a shear force is applied. To make contact, the tarsus is pulled toward the body (which automatically happens when the animal is hanging upside down), whereas elastic recoil helps to release the setae when the proximal pull is reduced or when the foot is moved distally (Fig. 2B). Negligible detachment forces in the absence of a proximal pull have been reported for gecko setae (Autumn et al., 2000). The second possible advantage of distally convex setae may be a greater resistance against self-matting. Even though distally convex setae have approximately the same flexibility in the vertical direction as proximally convex ones, the distance between setae is greater near the seta tips so that they may be less susceptible to self-matting.

Models of adhesion enhancement in hairy pads

Only recently, experiments conducted by Peressadko and Gorb demonstrated that adhesion can be increased for a block of the same material, when it is not smooth but patterned with high aspect ratio structures (hairs) (Peressadko and Gorb, 2004). Due to the smaller apparent contact area, the hairy surface had a greater tenacity (adhesive force per unit contact area). To explain the increase of adhesive forces achieved by hairy pad structures, three types of theoretical arguments have been proposed, which are based on different assumptions and are not fully compatible with each other.

(a) 'Fracture mechanics' argument

A fundamental concept in the field of fracture mechanics is the crack length. A crack will propagate in a block of material when the elastic energy released is greater than or equal to the increased energy associated with new surfaces. As the energy invested to create new surfaces is linearly related to crack length *CL*, whereas the gained elastic energy is proportional to its square, a crack propagates once its length exceeds a critical value given by the Griffith criterion (Griffith, 1921):

$$CL \geqslant \frac{2\gamma E}{\pi\sigma^2} \, , \qquad (2)$$

where σ is the applied stress, γ the surface energy, and E the elastic modulus of the material. Similar concepts have been applied to the detachment of adhesive setae (Gao et al., 2003; Gao and Yao, 2004; Hui et al., 2004). When the contact size is reduced to the range of the critical crack length or smaller, the adhesive strength increases and may come close to the maximum theoretical strength of the interface. When seta tips are larger, setae can detach by peeling (crack propagation), and the forces are expected to scale with contact radius. Even for larger setae, however, the shape of the tips can be optimised (by making them slightly concave) so that the stress is uniformly distributed over the contact zone (Gao and Yao, 2004). Under these conditions, the theoretical contact strength can be achieved, which is determined by the specific type of intermolecular interaction (for van der Waals forces ~20 MPa).
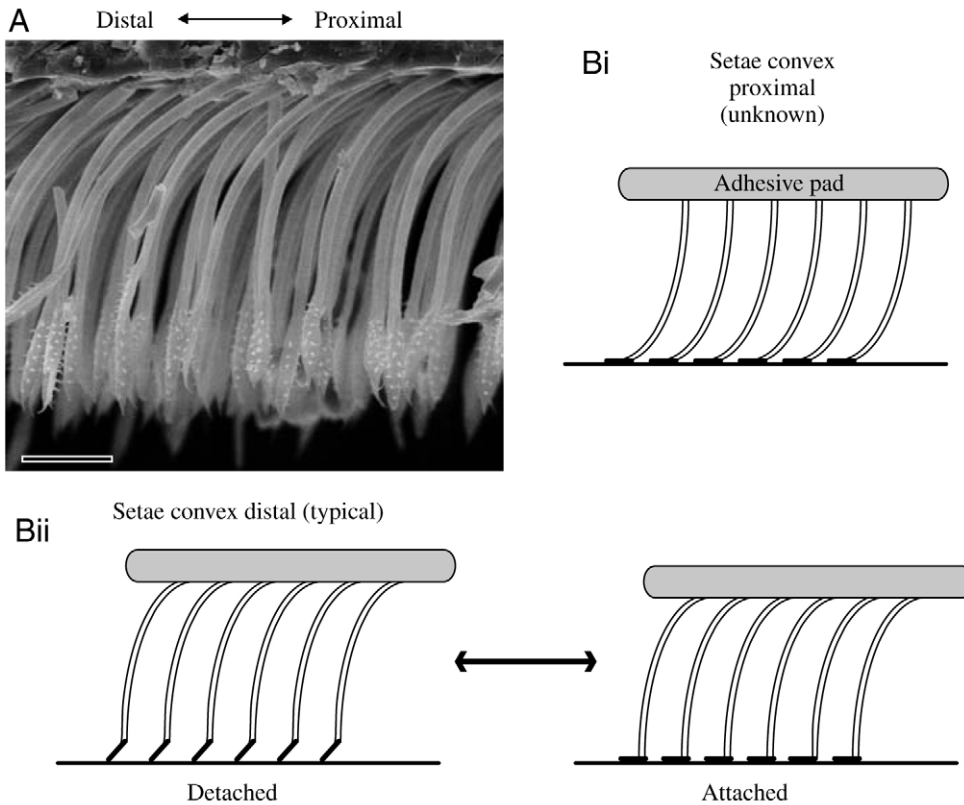
Fig. 2. Typical curvature of setae and control of attachment and detachment. (A) Lateral view of setae in the longhorn beetle *Clytus arietis*; note the vertical, non-adhesive orientation of the seta tips and the corrugations on the dorsal sides, which probably prevent self-matting. Scale bar, 20 μm. (B) Schematic diagrams of two possible seta orientations, convex proximal (Bi; not found in natural systems) and convex distal (Bii; typical orientation). Distally convex setae can easily switch between attachment and detachment by proximal and distal leg movements, respectively.

However, small departures from the optimal shape in larger setae strongly reduce adhesion. Adhesion becomes flaw-insensitive when the contact size is smaller than the Griffith crack length *CL* (Gao and Yao, 2004; Hui et al., 2004).

(b) 'Force scaling' argument

Contact mechanics models for the detachment of spheres, tapes and many other geometries predict adhesive forces to scale with length and not with area. This scaling relationship has given rise to the idea that adhesion can be increased by splitting up the contact zone into many subcontacts, because the total length of peeling edges increases. A greater number of (smaller) setae per pad area should thus increase overall adhesion (Arzt et al., 2003; Autumn et al., 2002; Spolenak et al., 2004). This concept has been used to explain the correlation of setal density with body size, because larger animals with relatively less available surface area (such as geckos) require a more effective adhesive system per unit attachment area than smaller animals such as insects (see Arzt et al., 2003; Spolenak et al., 2004).

One inherent assumption of this 'Force scaling' argument is that the pull-off stress is distributed uniformly over all the setae of a hairy pad (and that all bonds break simultaneously), so that the total adhesive force of a hairy pad is the product of the force of a single seta and the number of setae. However, this assumption will not hold when hairy pads detach from the surface by peeling so that stresses are concentrated at the edge of the pad. As only a small number of setae close to the peeling edge will 'share' the load (Hui et al., 2004), the pull-off force

of a pad will in this case be much smaller than that predicted by Force scaling. When peeling occurs, the critical measure for the sticking ability is not the adhesive force of a single fiber but the effective work of adhesion $W*$ of the fiber array (see below).

The question of whether hairy adhesive pads detach by peeling from the edge of the contact zone or by instantaneous detachment of all setae (load sharing) can be intuitively demonstrated by a simple experiment using Scotch^{TM} tape. Peeling a piece of Scotch^{TM} tape off a wall becomes much harder if a rigid plate is glued onto the (non-sticky) back side of the tape. While the peel force in the absence of the rigid plate scales with the width of the tape, a force proportional to the area of the rigid plate will be needed to peel off the modified tape. A theoretical analysis of the conditions under which the pull-off force is equally distributed over all setae of a pad (see Appendix) shows that not only the size of the pad, but also its flexibility and the dimensions and material properties of the 'backing' are important. Equal load sharing may be possible in very small pads, if the setae are very compliant and if the structures from which the setae emerge are very stiff.

(c) 'Work of adhesion' model

When an adhesive tape is pulled off a surface, the pull-off stress is concentrated along a narrow zone at the peeling edge. The peel force is proportional to the product of the width of the tape and the 'effective work of adhesion' $W*$ (i.e. the energy per unit area required to detach the tape from the surface). Both

in adhesive tape and in hairy adhesive pads, the surface energy needed to create two new interfaces is much smaller than the work required to bend and stretch the polymer or the fibers during detachment (Gay and Leibler, 1999; Persson, 2003). Due to the geometry of adhesive setae, most of this energy is not transmitted to neighboring fibers and is therefore lost upon detachment so that the fibers act as effective 'crack arresters' (Hui et al., 2004; Jagota and Bennison, 2002). By comparison, when a block of brittle material such as glass breaks, elastic strain energy is released at the crack tip and is transferred to the zone ahead of the crack, so that the crack can propagate.

As a consequence, the adhesion of a hairy pad mainly depends on the energy needed to detach a single seta. In the Appendix it is shown that the effective work of adhesion W^* of a setal array is given by:

$$W_\theta^* = \frac{F_0^2 N_A l}{2\pi r^2 E} \cdot g(\theta)$$

$$\text{where} \quad g(\theta) = \sin\theta \cdot \left[\frac{4}{3}\left(\frac{l}{r}\right)^2 \cos^2\theta + \sin^2\theta \right], \quad (3)$$

where θ is the angle of the seta with the surface, F_0 the adhesive force of one seta, N_A the number of setae per unit pad area, E the elastic modulus, r and l the radius and length of the seta, respectively. Eqn 3 takes into account that oblique setae come closer to each other and need to be spaced further apart (at least in the direction in which they are oriented) in order to avoid self-matting.

Can adhesion be increased by splitting contacts into finer subcontacts?

Contact mechanics models (e.g. Johnson et al., 1971) and the Griffith criterion predict that the adhesive strength (=force per contact area) of a single seta is increased when setae become smaller. This effect can continue until the maximum interfacial strength of the interface is reached. However, the 'Force scaling' and 'Work of adhesion' models differ with regard to the question of how this increase of adhesive strength translates into the adhesive force of an entire hairy pad. The 'Force scaling' model predicts that a pad with a dense cover of fine adhesive hairs achieves a greater adhesive force per pad area than an equally sized smooth pad or a pad that is less densely covered with coarser setae (Eqn 11). By contrast, a neutral effect or even a decline of forces with seta density is predicted from the 'Work of adhesion' model (Eqn 15). As a consequence, both models predict a different scaling relationship of adhesive hair density with the animal's body mass. According to the 'Force scaling' model, hair density should increase with body size, because larger animals with relatively less available surface area (such as geckos) require

a more effective adhesive system (Arzt et al., 2003; Spolenak et al., 2004). However, no such scaling effect would be predicted from the 'Work of adhesion' model, i.e. if hairy pads detach by peeling (see Appendix). Does the scaling of hair density with body mass disprove the 'Work of adhesion' model?

The 'Force scaling' model has been supported by data on the scaling of seta density with body mass from diverse animals (Arzt et al., 2003). A re-inspection of the data on seta density and body mass, however, suggests an alternative interpretation. Fig. 3 shows the data from Arzt et al.'s study (Arzt et al., 2003) together with one additional data point from a small spider, *Evarcha arcuata* (Kesel et al., 2003). This salticid spider's seta density is comparable to that of large spiders and lizards and is orders of magnitude higher than that of similar-sized insects. This distribution strongly indicates that animals with 'dry' adhesive systems (i.e. spiders and lizards) generally have pads with a much greater density of setae (spatulae) than insects which use 'wet' adhesion. The differences of adhesive hair density observed in Fig. 3 thus might largely reflect the type of adhesive system rather than the proposed body size dependence. Moreover, seta density is probably a taxon-specific trait. Clearly, more data are needed to investigate for each taxon whether there is any correlation of seta density and body size.

The large difference in hair density between dry and wet adhesive systems is easily explained by the need to cope with small-scale surface roughness (see Appendix). Presumably, the very close surface contact required for dry adhesion can only be achieved with extremely fine terminal elements, whereas in wet adhesive systems, even larger setae tips can adhere well when substrate cavities are filled out with fluid (Fig. 4).

The high density of adhesive hair tips in spiders and lizards correlates with the presence of branched setae in these animals.
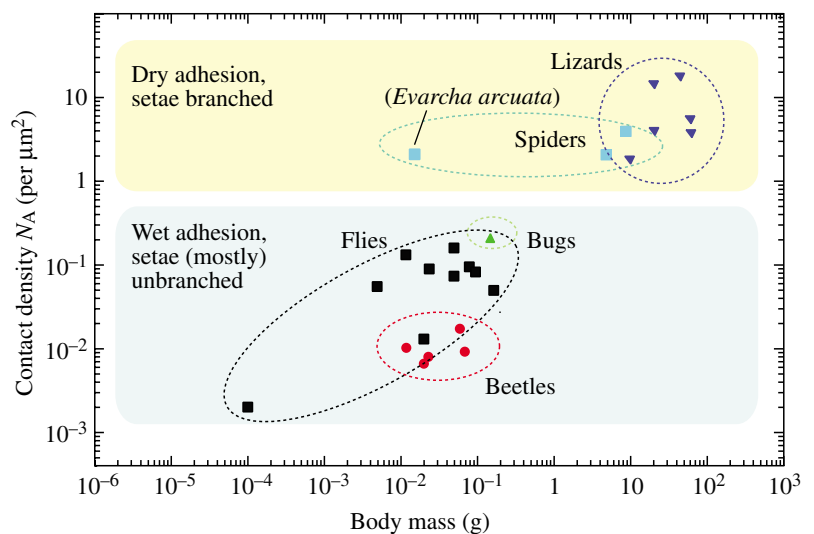

Fig. 3. Relationship between contact density (N_A) of hairy pads and body mass for animals from a variety of taxa. Data from the studies by Arzt et al. (Arzt et al., 2003) and Kesel et al. (Kesel et al., 2003) (only *Evarcha arcuata*).

The branched morphology may be necessary to achieve greater hair densities without sacrificing seta flexibility (Eqn 20). As shown in the Appendix, an array of branched setae can reach a greater work of adhesion than an array of similar-sized unbranched setae (Eqn 19).

Even though a general increase of seta density with body size due to 'Force scaling' is unlikely for the reasons given above, it may be no coincidence that the largest animals capable of running upside down, the geckos, use dry adhesion and possess branched setae with extremely fine seta tips. In dry adhesion, the maximum theoretical interfacial strength (for van der Waals forces ~20 MPa) is distinctly larger than in wet adhesion, where very negative capillary pressures are limited by fluid cavitation (~1 MPa) (Smith, 1991).

Conclusions and open questions

Hairy adhesive pads have convergently evolved in diverse animals. The hairy design may be biologically advantageous in several ways. It brings about the capacity to cope with surface roughness and pad contamination, and may help to achieve controllable detachment and increased adhesion. I have shown that many aspects of the morphological structure of hairy pads can be understood in the context of theoretical models of adhesion and avoidance of adhesion between setae. A detailed functional understanding of the hairy pad design and its manifold variations in biological systems has a great potential to provide insight leading to the development of novel technical adhesives and microgrippers, for which there would be numerous applications.

While considerable progress has been made over the last decade with respect to theoretical models of fibrillar adhesion and first attempts to fabricate biomimetic hairy adhesives, much more work remains to be done to improve our understanding of the biological systems. The detailed relationship between adhesive pad/seta structure and adhesive/frictional performance is still

Fine setae / spatulae

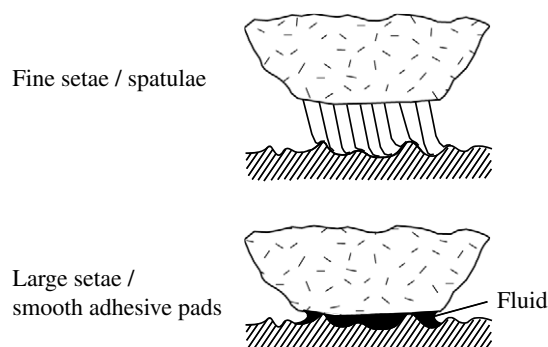Large setae / smooth adhesive pads — Fluid

Fig. 4. Schematic diagram illustrating two possible strategies of compensating small-scale surface roughness (roughness smaller than the dimensions of the pad). Good adhesive contact can either be achieved 'dry' with very fine seta tips or 'wet' by secretion of a fluid that can fill out substrate cavities. A fluid may not only be necessary in smooth adhesive pads (e.g. many insects and tree frogs) as shown here but also in hairy pads, when setae are relatively large and blunt as in many insects.

largely unclear. Moreover, it remains to be clarified whether and how the two principal adhesive pad designs found in nature, hairy and smooth pads, differ in their performance. Studies analyzing the forces generated by animal adhesive pads, as well as their dynamic behaviour during locomotion, and the scaling of pad structures and forces, will be essential to provide a more complete answer to the question of why so many adhesive pads are hairy.

Appendix
Conditions for the applicability of the 'Force scaling' vs 'Work of adhesion' models

One precondition for the 'Force scaling' hypothesis is that the pull-off force is distributed equally over all setae of a pad. This requires that the characteristic distance of stress decay from the peel edge must be substantially larger than the length of the pad contact area. It has been predicted that there is a characteristic length scale d (from the peeling edge inward), where the force decays to zero (Kaelble, 1960):

$$d = \left(\frac{E_B h_B^3 h_A}{3 E_A} \right)^{1/4}, \qquad (4)$$

where h_B and h_A are the thickness and E_B and E_A the elastic moduli of the backing and the adhesive, respectively. For an array of perpendicular adhesive hairs, a similar prediction has been derived (Hui et al., 2004):

$$d = \left(\frac{E_B h_B^3 l}{3 E_f N_A r^2 \pi} \right)^{1/4}. \qquad (5)$$

In order for the setae to share the load equally (a requirement for 'Force scaling'), the characteristic distance of stress decay from the peel edge must be substantially larger than the length of the pad contact area. To my knowledge, no data on the dimensions and material properties of the 'backing' in a hairy adhesive pad are available to test this. A crude estimate, assuming $E_B \approx E_f$, $N_A r^2 \pi \approx 0.1$ and $l \approx 10 h_B$ gives $d \approx 2 h_B$, which is probably orders of magnitude smaller than the dimensions of the adhesive pad. For sloped setae, however, the decay distance may be considerably greater ($d' = g(\theta)*d$, see Eqn 10). Thus, the 'Work of adhesion' model is more likely to be appropriate but it cannot be excluded that for sloped setae, the load is distributed over the entire pad.

According to the 'Fracture mechanics' argument, smaller size increases the tenacity of setae so that the force per contact area approaches the theoretical strength of adhesion. The scaling of adhesive forces with seta radius will therefore increase from approximately length-specific to area-specific scaling. As the 'Fracture mechanics' argument predicts forces only for individual setae, it is consistent with both other hypotheses.

Seta angle and effective work of adhesion W of hairy pad*

The effective work of adhesion W^* of a hairy pad is the product of the density of setae N_A (i.e. the number of setae per unit pad area) and the energy U needed to detach a single seta.

Assuming that a seta sticking to the surface with the force F, is bent or stretched normal to the substrate by δ_{max} before detachment, its energy of detachment U is:

$$U = \frac{F_0 \cdot \delta_{max}}{2} . \qquad (6)$$

The effective work of adhesion W^* of the seta array is $W^* = N_A \cdot U$, where N_A is the number of setae per unit pad area. The effective work of adhesion for an array of perpendicular fibers (where fiber deformation is only tensile) is (Gao et al., 2004; Hui et al., 2004; Jagota and Bennison, 2002; Persson, 2003):

$$W^*_{90°} = \frac{F_0^2 N_A l}{2\pi r^2 E} , \qquad (7)$$

where E is the elastic modulus, r and l the radius and length of the seta, respectively.

However, as long fibers are much more easily deformed tangential to the direction of the fiber (bending) than along their axis (stretching), arrays with oblique fibers are much more compliant and should have a much higher work of adhesion. Oblique fibers are displaced perpendicular to the surface (Glassmaker et al., 2004; Persson, 2003; Sitti and Fearing, 2003) by:

$$\delta_{max} = \delta_{bending} \cos\theta + \delta_{compress/tensile} \sin\theta =$$

$$\frac{4l^3 F_0 \cos^2\theta}{3\pi r^4 E} + \frac{F_0 l \sin^2\theta}{\pi r^2 E} , \qquad (8)$$

where θ is the seta angle. Combination of Eqn 6 and 8 gives:

$$U = \frac{F_0^2 l}{2\pi r^2 E} \cdot \left[\frac{4}{3} \left(\frac{l}{r} \right)^2 \cos^2\theta + \sin^2\theta \right]. \qquad (9)$$

Thus, the detachment energy becomes considerably larger for angles smaller than 90° and can be orders of magnitude greater for higher seta aspect ratios ($l/2r$) and smaller angles. However, the advantage of non-perpendicular fibers could be nullified by the fact that oblique fibers come closer to each other and may need to be spaced further apart (in the direction in which they are oriented) in order to avoid self-matting. This pattern is indeed observed in some insects (Fig. 1A). Thus, if N_A is the maximal number of perpendicular fibers per unit area permitted by the self-matting condition (Eqn 1), only a smaller density of $N'_A = N_A \sin\theta$ is possible for sloped fibers. The angle-dependent work of adhesion W^*_θ of the fiber array is then:

$$W^*_\theta = U \cdot N'_A = W^*_{90°} \cdot g(\theta) ,$$

$$\text{where} \quad g(\theta) = \sin\theta \cdot \left[\frac{4}{3} \left(\frac{l}{r} \right)^2 \cos^2\theta + \sin^2\theta \right]. \quad (10)$$

The function $g(\theta)$ is shown in Fig. 1B. It can be seen that

adhesion is maximised for an intermediate angle θ_{max}. For setae with a large fiber aspect ratio ($l/2r > 20$), W^*_θ scales with $\sin\theta \cos^2\theta$ and is maximal at $\theta_{max} = \arcsin(1/\sqrt{3}) \cong 35°$.

Scaling of seta density: predictions from the 'Force scaling' and 'Work of adhesion' models

(a) 'Force scaling'

The 'Force scaling' model assumes that all setae of a hairy pad share the load so that the total adhesive force of a hairy pad is the product of the force of a single seta and the number of setae. If the adhesive force of a single seta scales with its radius r, the force per area of the pad will increase with the number of setae per area:

$$\frac{F}{A} \propto \frac{1}{r} \propto \sqrt{N_A} . \qquad (11)$$

To compensate for the size-related loss of adhesive pad area, large animals are expected to increase the adhesive force per pad area by increasing the density of setae, leading to the prediction of $N_A \propto m^{2/3}$ (Arzt et al., 2003). Similar positive scaling coefficients have been predicted for other tip geometries (Spolenak et al., 2004).

(b) 'Work of adhesion' model

The effective work of adhesion W^* depends on several variables, according to Eqn 10:

$$W^*_\theta = \frac{F_0^2 N_A l}{2\pi r^2 E} \cdot g(\theta) \cong \sin\theta \cos^2\theta \cdot \frac{2 F_0^2 N_A l^3}{3\pi r^4 E} . \qquad (12)$$

Similar to the conclusions derived from the 'Force scaling' hypothesis (Arzt et al., 2003; Spolenak et al., 2004), Eqn 12 suggests that splitting up the contact into finer subcontacts can lead to increased adhesion. However, miniaturisation of the contacts is limited by the non-matting constraint (Spolenak et al., 2005). Assuming that the number of setae N_A is the maximum allowed by the non-matting condition (Eqn 1), Eqn 12 gives:

$$W^*_\theta = \sin\theta \cos^2\theta \cdot \frac{3\pi}{32} \frac{r^4 E}{l^3} . \qquad (13)$$

In the non-matting condition (Eqn 1), the adhesive force of a single seta F_0 is expected to scale with r^k [$1 \leq k \leq 2$, depending on the contact shape and dimensions (Hui et al., 2004; Spolenak et al., 2004)]. Assuming that the area fraction covered by setae $N_A \cdot r^2 \pi$ remains constant, Eqn 1 yields the following proportionalities:

$$N_A \propto \begin{cases} E^{\frac{1}{2}} l^{-\frac{3}{2}} & \text{if} \quad F_0 \propto r \\ E^{\frac{2}{3}} l^{-2} & \text{if} \quad F_0 \propto r^2 \end{cases} . \qquad (14)$$

Thus, increasing the number of setae per area requires shorter setae and/or a harder material. If setae are unbranched, this will not only reduce the flexibility of the hairy pad but also

impose a limit to the work of adhesion. For the two limiting cases of $F \propto r$ and $F \propto r^2$, combination of Eqn 13 with the proportionalities of Eqn 14 yields:

$$W_\theta^* \propto \begin{cases} El^3E^{-1}l^{-3} \propto (N_A)^0 \text{ (i.e. invariant)} & \text{if } F_0 \propto r \\ El^4E^{-\frac{4}{3}}l^{-3} \propto (N_A)^{-\frac{1}{2}} & \text{if } F_0 \propto r^2 \end{cases}. \quad (15)$$

Eqn 15 indicates that the effective work of adhesion cannot be increased by a greater number of setae per area N_A, because this would require the setae to be shorter and stiffer, which in turn would result in a reduction of the effective work of adhesion. As a consequence, no positive scaling of hair density with body mass is expected, in contrast to the predictions derived from the 'Force scaling' model (Arzt et al., 2003; Spolenak et al., 2004).

This conclusion holds only for unbranched setae. If, however, setae are branched as in spiders and geckos and some beetles, individual spatulae are effectively shorter and can be arranged at greater densities. Branching probably represents a strategy to prevent self-matting without sacrificing the work of adhesion.

Effect of seta branching

To investigate the effect of branched setae on the work of adhesion, a simplified model is considered (Fig. 5). Let us assume that every single seta of length L branches out into k spatulae of length l and identical angle θ [e.g. in geckos, k ranges between 100 and 1000, L/l may be of the order of 20 (Ruibal and Ernst, 1965)]. Multiple, hierarchical branching is ignored here. The cross-sectional area of a seta ($\sim R^2\pi$) is supposed to equal k times the cross-sectional area of the spatula stalks ($\sim r^2\pi$) so that $R \approx r \cdot \sqrt{k}$. As self-matting may only occur between spatulae but not between seta branches, the maximum density of setae N_A is k times smaller than the maximum density of spatulae n_A. It is further assumed that the load is shared equally among the spatulae of one seta (Hui et al., 2004), so that the adhesive force of one seta equals $k \cdot F_0$, where
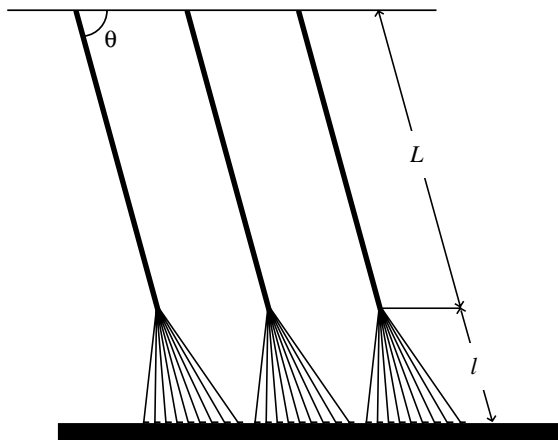
F_0 is the adhesive force of a single spatula. If $L \gg l$, the effective work of adhesion W^* is dominated by the loss of seta bending energy. W^* of an array of branched setae can be calculated by analogy with Eqn 12:

$$W_{\theta\text{(branched)}}^* \cong \sin\theta\cos^2\theta \cdot \frac{2(k \cdot F_0)^2(n_A/k) \cdot L^3}{3\pi(\sqrt{k} \cdot r)^4 E}. \quad (16)$$

If n_A is the maximum density of spatulae allowed by the non-matting condition (Eqn 1), this results in:

$$W_{\theta\text{(branched)}}^* = \sin\theta\cos^2\theta \cdot \frac{3\pi}{32} \frac{r^4 E L^3}{kl^6}. \quad (17)$$

For comparison, W^* of an array of unbranched setae (of the same diameter) would be (Eqn 13):

$$W_{\theta\text{(unbranched)}}^* \leqslant \sin\theta\cos^2\theta \cdot \frac{3\pi}{32} \frac{(\sqrt{k} \cdot r)^4 E}{L^3}, \quad (18)$$

thus,

$$W_{\theta\text{(branched)}}^* = W_{\theta\text{(unbranched)}}^* \cdot \frac{(L/l)^6}{k^3}. \quad (19)$$

Eqn 19 predicts that if $(L/l)^2 > k$ (i.e. for moderate numbers of relatively short spatulae), the work of adhesion of an array of branched setae can strongly exceed that of an array of unbranched setae with the same tip size. The underlying assumptions of Eqn 17 may be oversimplified (e.g. N_A is probably not only determined by the spatulae but also by the seta geometry) so that the amount of W^* gained by branching is probably overestimated. However, the model is useful to demonstrate the basic effect.

The combination of Eqn 15 and Eqn 19 shows that, according to the 'Work of adhesion' model, the splitting of adhesive contacts into finer subcontacts can only lead to increased adhesion if branched setae are introduced. Thus, the branched morphology of setae in lizards, spiders and some beetles may not only be important for making contact to surfaces with roughness at different length scales (Persson, 2003) but also for preventing self-matting and thus maximising adhesion.

Rough surface compatibilty and wet adhesion

To achieve sufficient contact to a rough substrate, an adhesive pad must be able to conform to the surface profile at different length scales (Persson, 2003). In hairy adhesive pads, two conditions must be satisfied: (1) the underlying tissue, the setae (and the spatulae) must be compliant enough so that the array can follow the large-scale (and intermediate scale) surface height profile, and (2) terminal elements must be very small and/or very flexible to compensate for smaller scale roughness.

If the surface roughness amplitude is larger than the maximum deflection δ_{max} of a single seta, an array can only

Fig. 5. Model used to estimate the effect of seta branching. For an explanation of symbols, see List of symbols.

make full contact by compressing some setae (those in contact with the highest peaks), which will store elastic energy and will reduce the total adhesive force. Thus, good adhesion may be achieved by making setae very compliant so that δ_{max} exceeds the surface roughness amplitude. Since $W_A \propto \delta_{max}$, this would also result in a greater work of adhesion. However, because of the tendency of setae to stick to each other (Eqn 1), seta flexibility (Eqn 8) can only be increased at the cost of reducing the number of setae per area (N_A):

$$\delta_{max} \cong \frac{4l^3 F_0 \cos^2\theta}{3\pi r^4 E} \propto (N_A)^{-\frac{1}{2}}. \qquad (20)$$

As shown above, this may be different if setae are branched. The branched seta morphology may not only prevent self-matting and increase the work of adhesion, but also brings along the advantage that setae can adapt to roughness at different length scales (Persson, 2003).

Even when setae are compliant enough to come into contact with the surface, small scale surface roughness (i.e. 'cavities' smaller than the size of a terminal element) can prohibit intimate contact and result in poor adhesion and friction. The fact that terminal elements are often extremely thin plates suggests that part of the small scale roughness is compensated by the flexibility of the terminal plate (Persson and Gorb, 2003). Not only the flexibility of the terminal elements, but also their absolute size is critical. The smaller a seta tip (terminal element), the wider the range of surface roughness length scales it can compensate.

A different mechanism is probably essential for providing sufficient attachment to rough substrates in species with larger adhesive setae and animals with smooth adhesive pads (many insects and treefrogs). Here, an 'adhesive' fluid is secreted into the contact zone, which can fill out the substrate cavities and provide enhanced adhesion (see Fig. 4). As 'dry' adhesion by van der Waals forces requires extremely close contacts (<10 nm), larger setae devoid of a fluid would achieve only poor adhesion on substrates with roughness at length scales smaller than the width of the seta. All animals using dry adhesion (i.e. spiders and lizards) possess extremely fine adhesive hairs, indicating that seta miniaturisation is essential for dry adhesion.

List of symbols

θ	seta angle
δ_{max}	maximum deflection
E	elastic modulus
F_0	adhesive force of unbranched seta or spatula
k	number of spatulae per seta
L	length of branched seta
l	length of unbranched seta or spatula
m	body mass
N_A	number of setae per unit pad area
n_A	number of spatulae per unit pad area
r	cross-sectional radius of seta
U	energy of seta detachment
W^*	effective work of adhesion

References

Arzt, E., Gorb, S. and Spolenak, R. (2003). From micro to nano contacts in biological attachment devices. *Proc. Natl. Acad. Sci. USA* **100**, 10603-10606.

Autumn, K. and Peattie, A. M. (2002). Mechanisms of adhesion in geckos. *Integr. Comp. Biol.* **42**, 1081-1090.

Autumn, K., Liang, Y. A., Hsieh, S. T., Zesch, W., Chan, W. P., Kenny, T. W., Fearing, R. and Full, R. J. (2000). Adhesive force of a single gecko foot-hair. *Nature* **405**, 681-685.

Autumn, K., Sitti, M., Liang, Y. A., Peattie, A. M., Hansen, W. R., Sponberg, S., Kenny, T. W., Fearing, R., Israelachvili, J. N. and Full, R. J. (2002). Evidence for van der Waals adhesion in gecko setae. *Proc. Natl. Acad. Sci. USA* **99**, 12252-12256.

Betz, O. (2003). Structure of the tarsi in some *Stenus* species (Coleoptera, Staphylinidae): external morphology, ultrastructure, and tarsal secretion. *J. Morphol.* **255**, 24-43.

Beutel, R. G. and Gorb, S. N. (2001). Ultrastructure of attachment specializations of hexapods (Arthropoda): evolutionary patterns inferred from a revised ordinal phylogeny. *J. Zool. Syst. Evol. Res.* **39**, 177-207.

Briggs, G. A. D. and Briscoe, B. J. (1977). The effect of surface topography on the adhesion of elastic solids. *J. Phys. D Appl. Phys.* **10**, 2453-2466.

Coddington, J. A. and Levi, H. W. (1991). Systematics and evolution of spiders (Araneae). *Annu. Rev. Ecol. Syst.* **22**, 565-592.

Dawkins, R. and Dawkins, M. (1976). Hierarchical organization and postural facilitation: rules for grooming in flies. *Anim. Behav.* **24**, 739-755.

de Crevoisier, G., Fabre, P., Corpart, J.-M. and Leibler, L. (1999). Switchable tackiness and wettability of a liquid crystalline polymer. *Science* **285**, 1246-1249.

Eisner, T. and Aneshansley, D. J. (2000). Defense by foot adhesion in a beetle (*Hemisphaerota cyanea*). *Proc. Natl. Acad. Sci. USA* **97**, 6568-6573.

Farish, D. J. (1972). The evolutionary implications of qualitative variation in the grooming behavior of the Hymenoptera (Insecta). *Anim. Behav.* **20**, 662-676.

Foelix, R. F. (1982). *The Biology of Spiders*. Cambridge, MA: Harvard University Press.

Fuller, K. N. G. and Tabor, D. (1975). The effect of surface roughness on the adhesion of elastic solids. *Proc. R. Soc. Lond. A* **345**, 327-342.

Gao, H. and Yao, H. (2004). Shape insensitive optimal adhesion of nanoscale fibrillar structures. *Proc. Natl. Acad. Sci. USA* **101**, 7851-7856.

Gao, H., Ji, B., Jaeger, I. L., Arzt, E. and Fratzl, P. (2003). Materials become insensitive to flaws at nanoscale: lessons from nature. *Proc. Natl. Acad. Sci. USA* **100**, 5597-5600.

Gao, H., Ji, B., Buehler, M. J. and Yao, H. (2004). Flaw tolerant bulk and surface nanostructures of biological systems. *Mech. Chem. Biosyst.* **1**, 37-52.

Gao, H., Wang, X., Yao, H., Gorb, S. and Arzt, E. (2005). Mechanics of hierarchical adhesion structures of gecko. *Mech. Mat.* **37**, 275-285.

Gay, C. and Leibler, L. (1999). Theory of tackiness. *Phys. Rev. Lett.* **82**, 936-939.

Geim, A. K., Dubonos, S. V., Grigorieva, I. V., Novoselov, K. S., Zhukov, A. A. and Shapoval, S. Y. (2003). Microfabricated adhesive mimicking gecko foot-hair. *Nat. Mat.* **2**, 461-463.

Glassmaker, N. J., Jagota, A., Hui, C.-Y. and Kim, J. (2004). Design of biomimetic fibrillar interfaces: 1. Making contact. *J. R. Soc. Interface* **1**, 23-33.

Gorb, S. N. (1998). The design of the fly adhesive pad: distal tenent setae are adapted to the delivery of an adhesive secretion. *Proc. R. Soc. Lond. B Biol. Sci.* **265**, 747-752.

Gorb, S. (2001). *Attachment Devices of Insect Cuticle*. Dordrecht, Boston: Kluwer Academic Publishers.

Gorb, S., Jiao, Y. and Scherge, M. (2000). Ultrastructural architecture and mechanical properties of attachment pads in *Tettigonia viridissima* (Orthoptera Tettigoniidae). *J. Comp. Physiol. A* **186**, 821-831.

Griffith, A. A. (1921). The phenomena of rupture and flow in solids. *Philos. Trans. R. Soc. Lond. A* **221**, 163.

Haas, F. and Gorb, S. (2004). Evolution of locomotory attachment pads in the Dermaptera (Insecta). *Arthropod Struct. Dev.* **33**, 45-66.

Hansen, W. R. and Autumn, K. (2005). Evidence for self-cleaning in gecko setae. *Proc. Natl. Acad. Sci. USA* **102**, 385-389.

Hooke, R. (1665). *Micrographia*. London: John Bowles.

Hui, C.-Y., Glassmaker, N. J., Tang, T. and Jagota, A. (2004). Design of biomimetic fibrillar interfaces: 2. Mechanics of enhanced adhesion. *J. R. Soc. Interface* **1**, 35-48.

Irschick, D. J., Austin, C. C., Petren, K., Fisher, R. N., Losos, J. B. and Ellers, O. (1996). A comparative analysis of clinging ability among pad-bearing lizards. *Biol. J. Linn. Soc. Lond.* **59**, 21-35.

Jagota, A. and Bennison, S. J. (2002). Mechanics of adhesion through a fibrillar microstructure. *Integr. Comp. Biol.* **42**, 1140-1145.

Johnson, K. L., Kendall, K. and Roberts, A. D. (1971). Surface energy and the contact of elastic solids. *Proc. R. Soc. Lond. A* **324**, 301-313.

Kaelble, D. H. (1960). Theory and analysis of peel adhesion: bond stresses and distributions. *Trans. Soc. Rheol.* **4**, 45-73.

Kesel, A. B., Martin, A. and Seidl, T. (2003). Adhesion measurements on the attachment devices of the jumping spider *Evarcha arcuata*. *J. Exp. Biol.* **206**, 2733-2738.

Khongtong, S. and Ferguson, G. S. (2002). A smart adhesive joint: entropic control of adhesion at a polymer/metal interface. *J. Am. Chem. Soc.* **124**, 7254-7255.

Langer, M. G., Ruppersberg, J. P. and Gorb, S. (2004). Adhesion forces measured at the level of a terminal plate of the fly's seta. *Proc. R. Soc. Lond. B Biol. Sci.* **271**, 2209-2215.

Lefebvre, L. (1981). Grooming in crickets: timing and hierarchical organisation. *Anim. Behav.* **29**, 973-984.

Niederegger, S., Gorb, S. and Jiao, Y. (2002). Contact behaviour of tenent setae in attachment pads of the blowfly *Calliphora vicina* (Diptera, Calliphoridae). *J. Comp. Physiol. A* **187**, 961-970.

Northen, M. T. and Turner, K. L. (2005). A batch fabricated biomimetic dry adhesive. *Nanotechnology* **16**, 1159-1166.

Paine, S. (2000). Want to walk on the ceiling? All it takes is a bit of fancy footwork. *New Sci.* **168**, 62-67.

Peressadko, A. and Gorb, S. N. (2004). When less is more: experimental evidence for tenacity enhancement by division of contact area. *J. Adhes.* **80**, 247-261.

Persson, B. N. J. (2003). On the mechanism of adhesion in biological systems. *J. Adhes. Sci. Technol.* **118**, 7614-7620.

Persson, B. N. J. and Gorb, S. (2003). The effect of surface roughness on the adhesion of elastic plates with application to biological systems. *J. Chem. Phys.* **119**, 11437-11444.

Pohl, H. and Beutel, R. G. (2004). Fine structure of adhesive devices of Strepsiptera (Insecta). *Arthropod Struct. Dev.* **33**, 31-43.

Power, H. (1664). *Experimental Philosophy*. London: Martin and Allestry.

Rovner, J. S. (1978). Adhesive hairs in spiders: behavioral functions and hydraulically mediated movement. *Symp. Zool. Soc. Lond.* **42**, 99-108.

Ruibal, R. and Ernst, V. (1965). The structure of the digital setae in lizards. *J. Morphol.* **117**, 271-294.

Sitti, M. and Fearing, R. S. (2003). Synthetic gecko foot-hair micro/nano-structures as dry adhesives. *J. Adhes. Sci. Technol.* **17**, 1055-1073.

Smith, A. M. (1991). Negative pressure generated by octopus succers: a study of the tensile strength of water in nature. *J. Exp. Biol.* **157**, 257-271.

Spolenak, R., Gorb, S., Gao, H. and Arzt, E. (2004). Effects of contact shape on the scaling of biological attachments. *Proc. R. Soc. Lond. A* **460**, 1-15.

Spolenak, R., Gorb, S. and Arzt, E. (2005). Adhesion design maps for bio-inspired attachment systems. *Acta Biomater.* **1**, 5-13.

Stork, N. E. (1980a). Experimental analysis of adhesion of *Chrysolina polita* (Chrysomelidae: Coleoptera) on a variety of surfaces. *J. Exp. Biol.* **88**, 91-107.

Stork, N. E. (1980b). A scanning electron microscope study of tarsal adhesive setae in the Coleoptera. *Zool. J. Linn. Soc.* **68**, 173-306.

Stork, N. E. (1983a). The adherence of beetle tarsal setae to glass. *J. Nat. Hist.* **17**, 583-597.

Stork, N. E. (1983b). A comparison of the adhesive setae on the feet of lizards and arthropods. *J. Nat. Hist.* **17**, 829-835.

Walker, G., Yule, A. B. and Ratcliffe, J. (1985). The adhesive organ of the blowfly, *Calliphora vomitoria*: a functional approach (Diptera: Calliphoridae). *J. Zool. Lond. A* **205**, 297-307.

Williams, E. E. and Peterson, J. A. (1982). Convergent and alternative disigns in the digital adhesive pads of scincid lizards. *Science* **215**, 1509-1511.

Yurdumakan, B., Raravikar, N. R., Ajayan, P. M. and Dhinojwala, A. (2005). Synthetic gecko foot-hairs from multiwalled carbon nanotubes. *Chem. Comm.* **2005**, 3799-3801.